Supporting information

General synthetic details

All syntheses were carried out using standard Schlenk and glove-box techniques, using an inert atmosphere of argon. Hexane was dried by refluxing over molten potassium, distilled and degassed by freeze-pump-thaw cycles prior to use. Deuterated NMR solvents (toluene-d_8 and benzene-d_6) were dried by refluxing over potassium before vacuum transferring to a J. Young's ampoule. NMR spectra were acquired on Bruker Avance-III 400 MHz or 500 MHz spectrometers. X-ray diffraction data were collected on a Oxford Instruments XCalibur2 diffractometer using MoKα radiation. Elemental analyses were carried out by Mr. Stephen Boyer at London Metropolitan University, U.K. Literature procedures were used to synthesize 1,3-bis(2,6-diisopropylphenyl)-1,3-diaza-2-silacyclopent-4-en-2-ylidene (^{Si}IPr) and [V(Cp)$_2$].[1,2]

Synthesis of [(^{Si}IPr)V(Cp)$_2$] (1)

A pale yellow solution of ^{Si}IPr (81 mg, 0.20 mmol) in hexane (5 ml) was slowly added to a purple solution of [V(Cp)$_2$] (36 mg, 0.20 mmol) in hexane (5 ml) at –78°C, producing a dark red solution. The reaction mixture was slowly warmed to room temperature, stirred for one hour, filtered, concentrated to a volume of ca. 3 ml, and stored at –30 °C. A batch of crystalline material formed after 24 hours. The crystals were collected, washed with hexane (2 × 5 ml) that had be pre-cooled to –78°C and dried under vacuum. Yield 83.0 mg (71 %). Anal. calcd. for $C_{36}H_{44}N_4SiV$: C 74.07; H 7.60; N 4.80. Found: C 73.96; H 7.68; N 4.85. ^{1}H NMR (500.19 MHz, toluene-d_6, δ/ppm, 238 K): (7.72 (4H, iPr-C*H*); 6.77 (6H, aryl C*H*); 3.72 (2H, ^{Si}IPr backbone); 1.31 (24H, iPr-C*H*$_3$); -0.20 (10H, cyclopentadienyl C*H*).

Spectral data

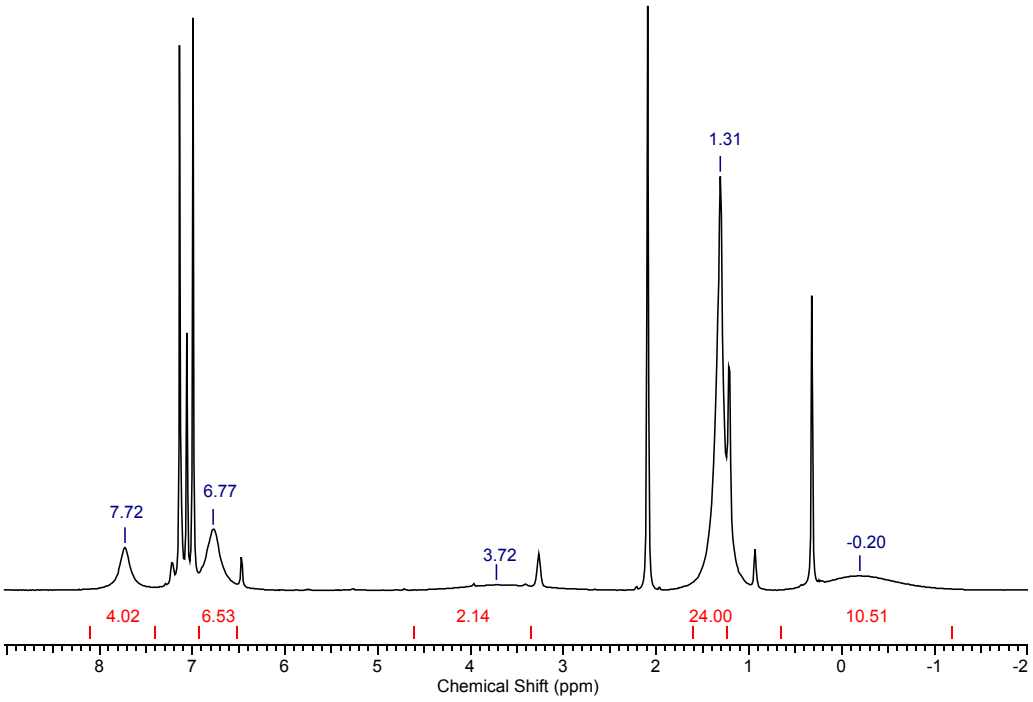

Figure S1. ^{1}H NMR spectrum of **1** in toluene-D_8 at 238 K.

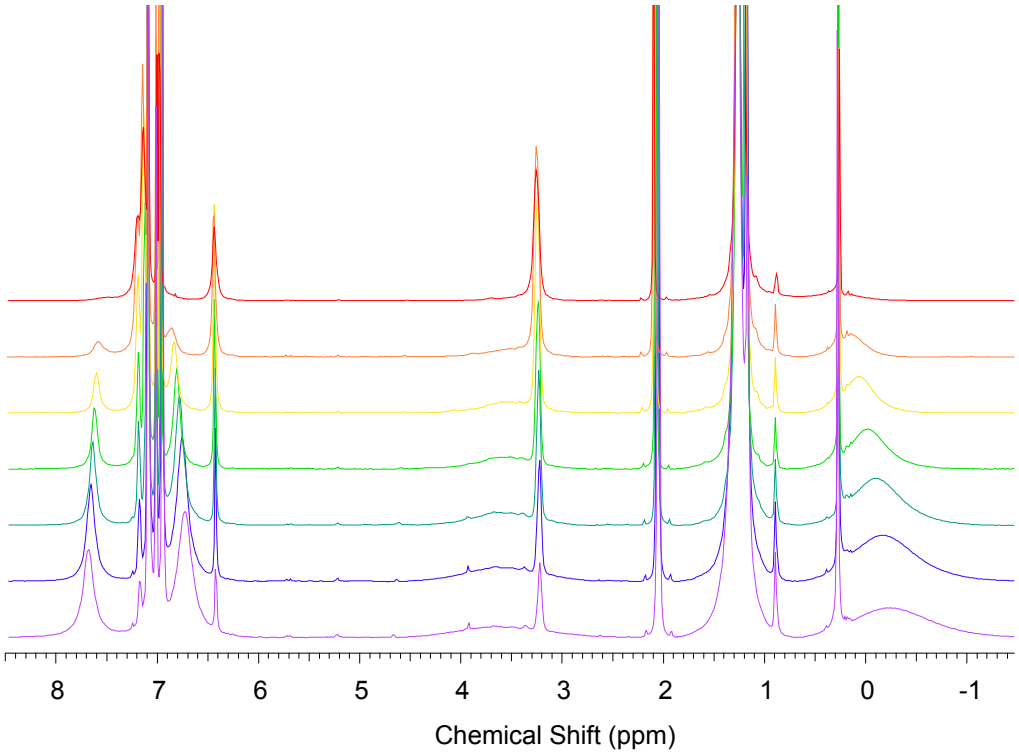

Figure S2. ^{1}H NMR spectrum of **1** in the range 238-333 K in toluene-D_8 (zoomed in).

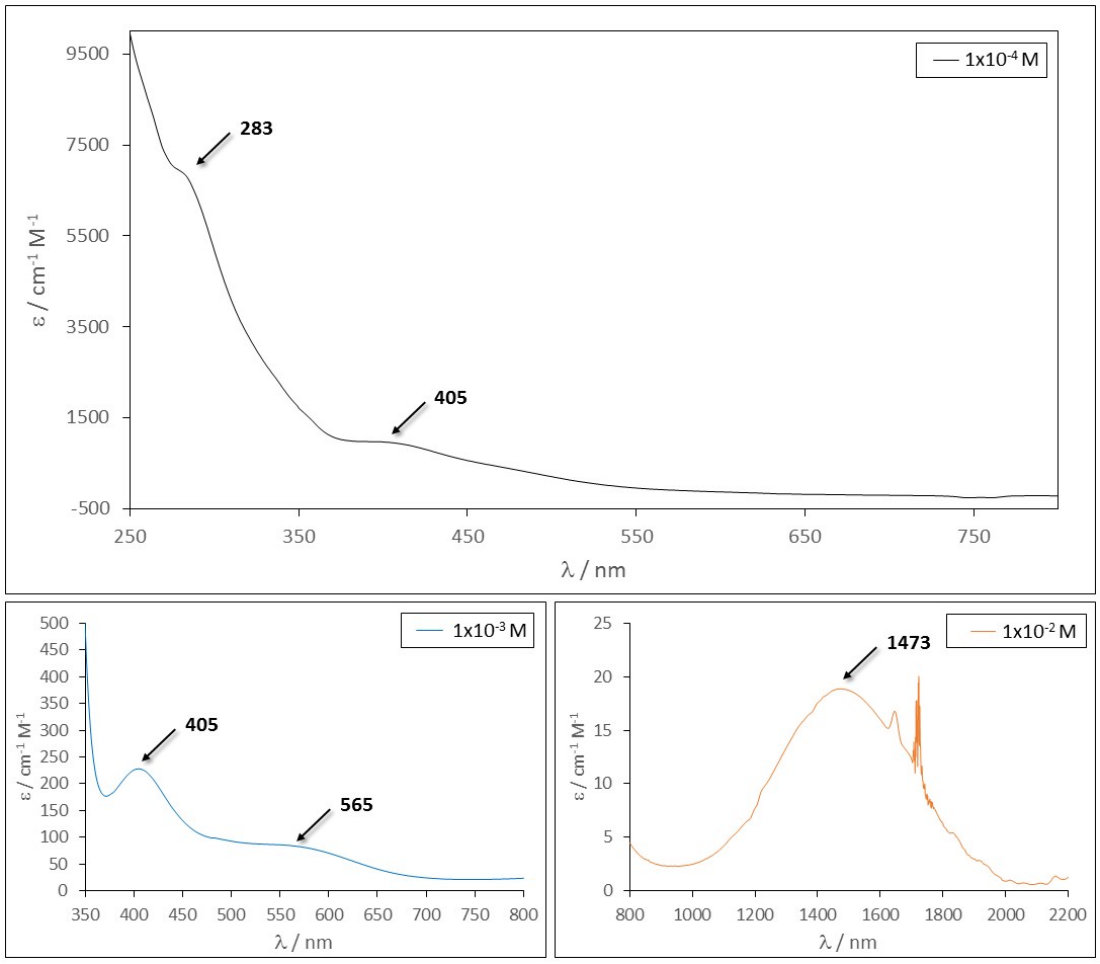

Figure S3. UV-VIS-NIR spectra of **1** in different concentrations in hexane.

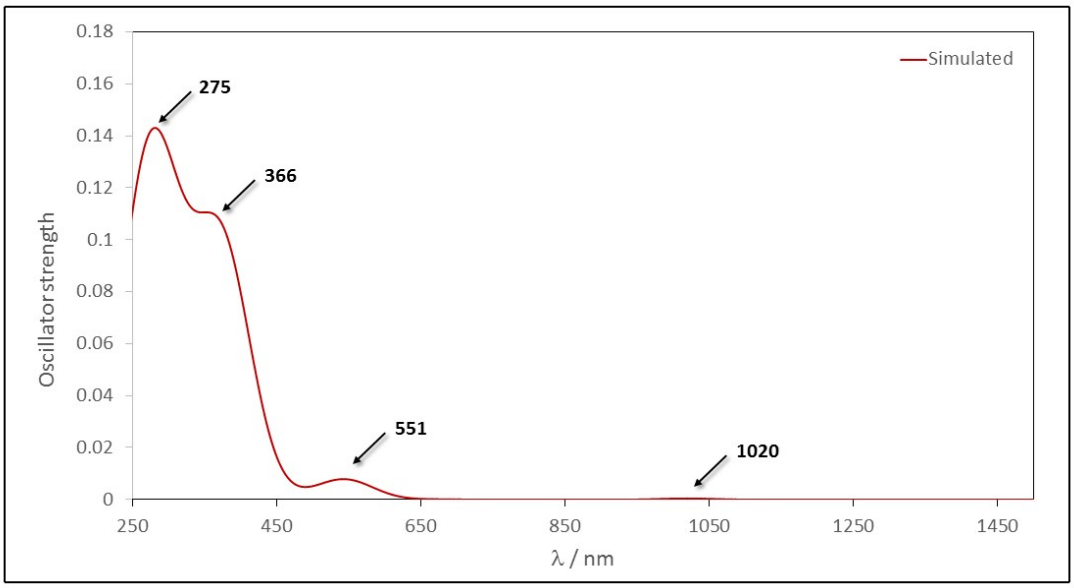

Figure S4. Simulated UV-VIS-NIR spectrum of **1** from TD-DFT [PBE0/def2mix, COSMO (hexane)] calculated oscillator strengths using Gaussian function and full-width half-maximum value of 90 (obtained from transition at 405 nm in the experimental spectrum).

Magnetic property measurements

The static magnetic properties of polycrystalline sample of **1** were measured using a Quantum Design MPMS-7 SQUID magnetometer at temperatures in the range 2-300 K. In a glove box, the polycrystalline sample was transferred to an NMR tube, restrained in eicosane and flame sealed under vacuum. The magnetic susceptibility and magnetization data were fitted simultaneously, using following Hamiltonian (Eq . 1) and the PHI software.[3] The best fit was found with S = ½ and g_{iso} = 1.90.

$$\hat{H} = \mu_B g \hat{S} \cdot \vec{B} \qquad (1)$$

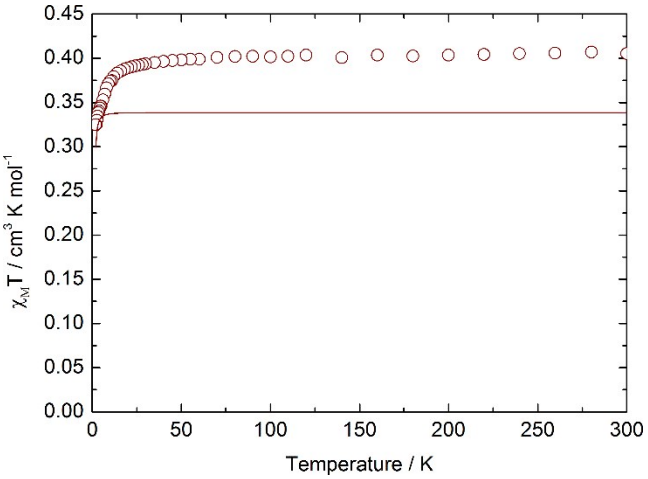

Figure S5. $\chi_M T$ vs T for **1** in an applied field 10 kOe.

X-ray diffraction

Table S1. Crystal data and structure refinement for **1**.

CCDC ref. code	1485743
Empirical formula	$C_{36}H_{46}N_2Si_1V_1$
Formula weight	585.78
Temperature/K	150
Crystal system	triclinic
Space group	$P\bar{1}$
a/Å	10.15070(15)
b/Å	18.9014(6)
c/Å	18.9172(6)
α/°	117.978(3)
β/°	90.4725(19)
γ/°	91.1512(19)
Volume/Å^3	3204.02(18)
Z	4
ρ_{calc} / g cm^{-3}	1.214
μ/mm^{-1}	0.374
F(000)	1252
Crystal size/mm^3	0.4 × 0.5 × 0.5
Radiation	Mo-K_α (λ = 0.71073 Å)
2θ range for data collection/°	6.622 to 58.166
Reflections collected	65256
Independent reflections	15096 [R_{int} = 0.0517, R_{sigma} = 0.0446]]
Data/restraints/parameters	15096/0/737
Goodness-of-fit on F^2	1.089
Final R indexes [I>2σ(I)]	R_1 = 0.0636, wR_2 = 0.1641
Final R indexes [all data]	R_1 = 0.0784, wR_2 = 0.1724
Largest diff. peak/hole / e Å^{-3}	1.36/–0.67

EPR studies

Continuous wave EPR measurements

The continuous wave EPR spectra were recorded on a Bruker EMX spectrometer operating X-band with a microwave frequency of ~ 9.4 GHz. The microwave frequency and magnetic field were measured using the Bruker internal frequency counter and field controller, respectively. In order to avoid a saturation of signals, an optimized microwave power of 0.2 – 0.5 mW (26 – 30 dB) was used for all experiments. Modulation amplitude of 2 – 5 G was applied to prevent an artificial signal broadening, combined with a fixed modulation frequency of 100 KHz applying a receiver gain of 1×10^4 - 1×10^5 depending upon the signal-to-noise ratio. A Bruker ESR900 helium cryostat was used for low temperature measurements. The applied magnetic field was calibrated using a Bruker standard sample with a well-known g-value.

Numerical spectrum simulations

In the numerical spectrum simulations of the vanadium complex, high-field conditions, i.e. $\beta_e\mathbf{B_0} \cdot \mathbf{g} \cdot \mathbf{S} >> h\mathbf{S} \cdot \mathbf{A} \cdot \mathbf{I}$, were assumed so that the effects of the nuclear field on the alignment of the electron spin are negligible, thus the electron problem can be treated independently. The hyperfine interaction is treated as a perturbation of the electron Zeeman energy. The corresponding energy levels are well-separated, and an m_S becomes a main quantum number. The coaxial orientation of g and A is assumed for the simulation. The EasySpin computational simulation package was used,[4] especially for refining of isotropic g factor and hyperfine interaction A tensor.

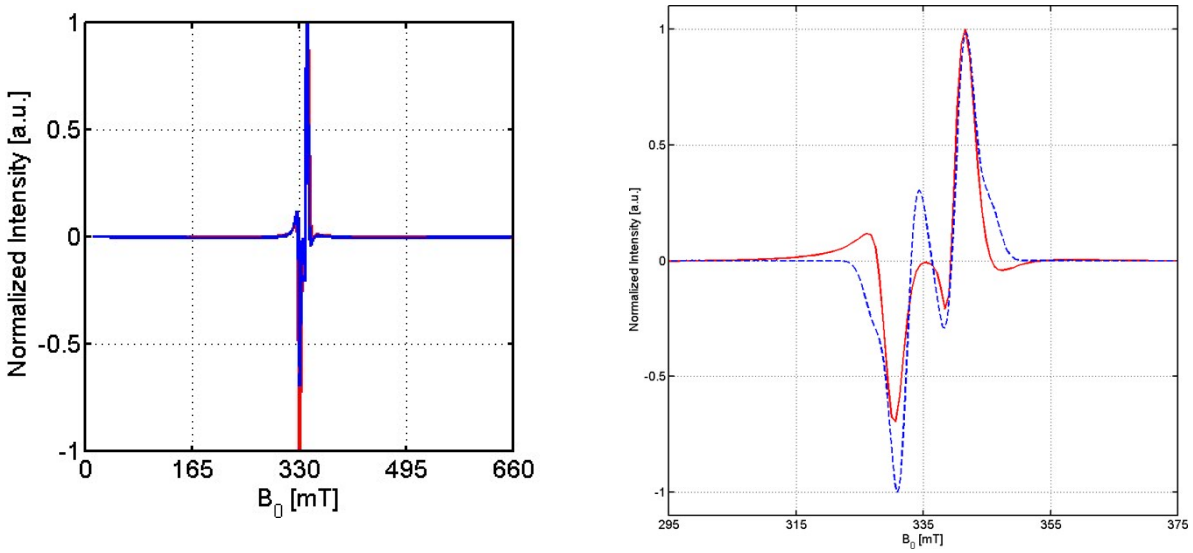

Figure S6. The X-band EPR spectra of vanadium-silylene (frozen solution de-gassed and sealed in a tube) were measured at 10 and 20 K. Left: Broad field scan. Right: The numerical simulation considering isotropic exchange coupling between the two neighboring S = ½ ions, according to $H = -2J_{ij}\mathbf{S}_i \cdot \mathbf{S}_j$. *The* A term in $\mathbf{S}_i \cdot \mathbf{S}_j$ is part of the dipolar interaction, and the effect of isotropic exchange (J = 84 MHz) is simply that of combining with dipolar couplings to the total spin-Hamiltonian.

Additional notes

The dipolar (anisotropic) coupling is averaged away, including the fine structure (zero-field splitting). In the non-relativistic limit, A_{iso} arises from Fermi contact term which is directly proportional to the spin density at the nucleus under consideration. It implies that A_{iso} is independent of molecular orientation as s-orbital has a spherical symmetry. This hyperfine multiplet can be explained as a superposition of spectra of the vanadium nuclei with statistical distributions of the two isotopes. However, ^{51}V (I = 7/2) possess the largest natural abundance of 99.75% and has a nuclear magnetic moment which is 62% larger than that of ^{50}V (I = 6). In the experiment, the difference is not resolved, but contributes to the linewidth. In a case of the spin density delocalization, the unpaired electron has the density probability about the vanadium nucleus in the nodal plane of the singly-occupied molecular orbital (SOMO), such as d-orbital.

It is also worth of noting that the EPR spectra of related high-spin vanadium complexes were significantly in homogeneously broadened because of its S = 3/2 state and the dominant zero-field splitting of D ~ 2.84 cm^{-1} at lower temperatures.[5] Such a large spin-anisotropy is only accessible via high-frequency and high-field EPR experiments, and apparently way out of the excitation range of microwave energy available with our X-band EPR experiments since g-anisotropy has to be split by anisotropy of the zero-field splitting. Accordingly, the simulations with such a large splitting did not match and reproduce the observed transitions in the parallel ($g_{||}$) region of our spectrum. At lower temperatures, we did not observe any signal at the low-field, equivalent to the transition at $g_{\perp}$ of high-spin vanadium complexes.[5]

Computational details

All calculations were performed using Turbomole (versions 6.6 and 7.0), ADF2013 or Gaussian09 program packages.[6-8] Geometries were optimized with the PBE1PBE (PBE0) functional and the def2-SVP basis set for C, H, N, Si (amide ligand) atoms, and def2-TZVP for the Fe and Si (^{Si}IPr ligand) atoms. Full vibrational analysis was performed for all optimized structures to confirm that they represent a local minimum. Energy decomposition analysis (EDA) was performed as implemented in ADF2013 using PBE(GGA) functional and DZP basis set for C, H, N, Si (amide ligand) atoms and TZVP for Fe and (^{Si}IPr ligand) atoms. EDA and ETS-NOCV analyses were performed as implemented in ADF2013 program package.[7] Theoretical oscillator strengths of 50 first excitations were calculated with ADF2013 using time dependent density functional theory (TDDFT). Solvation effects were taken into account using COSMO solvation model as implemented. Simulated spectrum was generated using ADFSPECTRA tool with Gaussian function and full-width half-maximum value of 90 that was obtained from transition at 405 nm in the experimental spectrum. Wiberg

bond indices were calculated using Gaussian NBO version 5.9[9] as implemented in Gaussian09 program package.

XYZ coordinates:

[(^{Si}IPr)V(Cp)$_2$] – DOUBLET

PBE0 / Def2mix (S = 1/2)

NIMAG = 0

SCF + E(vib0): -2738.7191447

86

V	8.85983	1.81031	3.67007
Si	6.81461	2.59395	4.46645
N	6.29794	3.75223	5.69456
N	5.11140	2.32779	4.08984
C	4.02729	1.84943	1.94183
C	4.25744	3.08269	4.89252
H	3.17788	2.99163	4.78187
C	4.90986	3.86337	5.77773
H	4.45681	4.54284	6.49822
C	4.54123	1.39364	3.17833
C	7.75972	5.70341	5.97701
C	7.20050	4.28674	7.90972
C	7.95922	5.13908	8.72030
H	8.04480	4.92613	9.78896
C	6.51914	3.07998	8.53218
H	6.11563	2.47168	7.70783
C	3.46690	0.91355	1.06716
H	3.06631	1.24979	0.10764
C	3.41589	-0.43740	1.39192
H	2.98050	-1.15421	0.69125
C	8.51574	6.51418	6.82789
H	9.03689	7.38216	6.41973
C	4.04955	3.31781	1.55362
H	4.71529	3.83055	2.26572
C	10.68841	2.24712	4.85029
H	11.40148	3.01391	4.55023
C	4.47364	0.02728	3.53077
C	3.91528	-0.87033	2.61417
H	3.86288	-1.93199	2.87008
C	9.93608	1.69292	1.70202
H	11.00861	1.52118	1.62958
C	7.62250	6.04658	4.50370
H	7.54379	5.08853	3.96311
C	8.61313	6.24255	8.18940
H	9.20576	6.89393	8.83654
C	7.91292	2.75278	1.84978
H	7.15899	3.53617	1.80068
C	9.31104	2.95847	1.75913
H	9.81568	3.92392	1.75715
C	7.66756	1.33221	1.84598
H	6.69444	0.84865	1.80872
C	8.92980	0.68904	1.76543
H	9.09839	-0.38645	1.73112
C	4.96214	-0.49232	4.87058
H	5.35595	0.36980	5.43045
C	4.60292	3.54691	0.14601
H	5.58448	3.06949	0.00895
H	4.71638	4.62498	-0.04924
H	3.92810	3.14912	-0.62847
C	2.65986	3.94655	1.69278
H	1.93926	3.46526	1.01175
H	2.69120	5.01965	1.44543
H	2.26869	3.84827	2.71578
C	6.33612	6.83679	4.24635
H	5.44690	6.28335	4.58225
H	6.21683	7.04876	3.17145
H	6.35723	7.80106	4.77995
C	9.56382	2.44096	5.69229
H	9.30888	3.35580	6.22094
C	6.10798	-1.49063	4.70520
H	5.78570	-2.39323	4.16136
H	6.48606	-1.81443	5.68824
H	6.94217	-1.03468	4.15051
C	7.49944	2.20547	9.31711
H	8.36694	1.91550	8.70582
H	7.00116	1.28579	9.66255
H	7.88184	2.72239	10.21156
C	10.73809	0.87487	4.48517
H	11.48611	0.40857	3.84625
C	8.90679	1.16412	5.82930
H	8.06829	0.93754	6.48506
C	5.34079	3.49635	9.41654
H	5.67925	4.11556	10.26309
H	4.83333	2.61101	9.83156
H	4.59584	4.07938	8.85548
C	3.81395	-1.08142	5.69263
H	3.00845	-0.34607	5.83965
H	4.17112	-1.39778	6.68563
H	3.37449	-1.96498	5.20221
C	8.83352	6.77278	3.92575
H	8.93916	7.79468	4.32427
H	8.72907	6.86667	2.83363
H	9.76820	6.22892	4.13142
C	9.64151	0.21203	5.08144
H	9.39574	-0.84345	4.97308
C	7.09740	4.58210	6.53246

[(^{Si}IPr)V(Cp)$_2$] – QUARTET

PBE0 / Def2mix (S = 3/2)

SCF + E(vib0): -2738.7041931

NIMAG = 0

86

V	8.79096	1.78672	3.72292
Si	6.65263	2.70167	4.51685
N	6.12552	3.84987	5.72554
N	4.97211	2.39710	4.13855
C	4.01060	1.90711	1.93398
C	4.10275	3.14271	4.92325
H	3.02536	3.03250	4.80999

C	4.74243	3.95465	5.79781
H	4.27904	4.64720	6.49893
C	4.46653	1.45421	3.19335
C	7.50360	5.85257	6.02304
C	7.19027	4.28136	7.89271
C	8.00496	5.10023	8.68004
H	8.20577	4.81837	9.71619
C	6.57614	3.02817	8.49170
H	6.21312	2.41193	7.65371
C	3.53178	0.95846	1.02589
H	3.17715	1.28620	0.04609
C	3.50457	-0.39521	1.34286
H	3.13265	-1.12041	0.61500
C	8.32167	6.62930	6.85059
H	8.76723	7.54540	6.45431
C	3.99376	3.38106	1.56455
H	4.65815	3.90249	2.27259
C	10.87156	2.21798	4.88419
H	11.53737	3.02402	4.57504
C	4.42655	0.08613	3.53907
C	3.94693	-0.82183	2.58864
H	3.91349	-1.88615	2.83565
C	10.12809	1.65225	1.58335
H	11.21135	1.76266	1.55278
C	7.23875	6.30907	4.59942
H	6.52190	5.60160	4.15456
C	8.57229	6.26137	8.16654
H	9.21259	6.88290	8.79719
C	7.88973	2.14976	1.62571
H	6.94906	2.69205	1.55150
C	9.18731	2.71924	1.58507
H	9.41813	3.77895	1.47690
C	8.03029	0.74341	1.74779
H	7.21359	0.02215	1.77803
C	9.42102	0.44536	1.69454
H	9.85849	-0.55083	1.75873
C	4.84992	-0.42590	4.90478
H	5.18298	0.44224	5.49447
C	4.51543	3.65253	0.15270
H	5.50470	3.20276	-0.01681
H	4.60075	4.73702	-0.01772
H	3.83461	3.25943	-0.61865
C	2.58926	3.97091	1.73139
H	1.87555	3.48001	1.05012
H	2.58968	5.04786	1.49988
H	2.21014	3.84721	2.75584
C	6.58741	7.69291	4.56121
H	5.65742	7.71552	5.14929
H	6.34169	7.97432	3.52510
H	7.25621	8.47071	4.96304
C	9.77256	2.35167	5.77200
H	9.46801	3.26483	6.28332
C	6.03053	-1.39302	4.81190
H	5.77139	-2.29642	4.23681
H	6.34305	-1.71926	5.81656
H	6.89582	-0.91687	4.32509
C	7.58646	2.19096	9.27706
H	8.48588	1.97157	8.68321
H	7.13374	1.23334	9.57835
H	7.90929	2.69723	10.20061
C	10.98235	0.85951	4.51204
H	11.72213	0.43798	3.83411
C	9.17659	1.06957	5.91278
H	8.33233	0.81651	6.55302
C	5.36700	3.37287	9.36666
H	5.66612	4.00389	10.21923
H	4.90581	2.45777	9.77082
H	4.59590	3.91775	8.80296
C	3.66955	-1.05111	5.65213
H	2.83431	-0.34110	5.74957
H	3.97348	-1.36008	6.66477
H	3.28888	-1.94567	5.13362
C	8.51156	6.26383	3.75223
H	9.27803	6.95439	4.13924
H	8.29598	6.55462	2.71175
H	8.94433	5.25122	3.74039
C	9.90732	0.15947	5.10594
H	9.70082	-0.90609	5.00323
C	6.94965	4.66873	6.55523

[(IPr)V(Cp)$_2$] – DOUBLET

PBE0 / Def2mix (S = 1/2)

NIMAG = 0

SCF + E(vib0): -2738.7191447

86

V	8.52117	1.96268	3.81797
C	6.54916	2.69558	4.56040
N	6.27506	3.61236	5.56207
N	5.27304	2.35470	4.14283
C	4.27802	1.86730	1.95588
C	4.28814	3.02422	4.84822
H	3.23236	2.86364	4.65626
C	4.91711	3.81317	5.73959
H	4.52948	4.51000	6.47544
C	4.86268	1.39965	3.15233
C	7.83823	5.49448	5.79203
C	7.28564	4.09415	7.74308
C	8.12474	4.90196	8.52087
H	8.23058	4.69003	9.58711
C	6.50257	2.98679	8.43310
H	6.06492	2.34464	7.65228
C	3.82324	0.91675	1.03324
H	3.37843	1.25473	0.09469
C	3.92831	-0.44268	1.28669
H	3.57629	-1.16743	0.54851
C	8.67146	6.25746	6.61284
H	9.20467	7.11040	6.19059
C	4.07403	3.34137	1.63782
H	4.66052	3.92829	2.36246
C	10.43462	1.87324	4.86908
H	11.32215	2.40309	4.52857
C	4.92363	0.02144	3.45546
C	4.46604	-0.88112	2.49313
H	4.51883	-1.95195	2.69467
C	9.80433	2.33957	2.03515
H	10.88925	2.39561	2.09856
C	7.59940	5.89672	4.34886
H	7.48294	4.96040	3.78222
C	8.82424	5.96228	7.96429
H	9.48157	6.57361	8.58740
C	7.60776	2.93686	1.92581

H	6.70952	3.54741	1.93439
C	8.91660	3.44103	2.07015
H	9.19465	4.48413	2.19889
C	7.66060	1.52425	1.76825
H	6.82795	0.86126	1.55344
C	9.03180	1.15033	1.85511
H	9.42545	0.14546	1.71495
C	5.40503	-0.47107	4.80723
H	6.21710	0.20654	5.11174
C	4.55194	3.71776	0.23260
H	5.58344	3.38835	0.04424
H	4.50992	4.80994	0.09825
H	3.91101	3.27365	-0.54489
C	2.60313	3.73974	1.80557
H	1.96538	3.18770	1.09691
H	2.46875	4.81531	1.60990
H	2.22531	3.53300	2.81712
C	6.30535	6.70773	4.21693
H	5.42931	6.15177	4.58119
H	6.12057	6.96884	3.16248
H	6.37100	7.64719	4.78961
C	9.49592	2.35489	5.82527
H	9.53792	3.31044	6.33922
C	5.97921	-1.88420	4.77068
H	5.20288	-2.64378	4.58530
H	6.43613	-2.12990	5.74170
H	6.75146	-1.99001	3.99396
C	7.38052	2.10652	9.32697
H	8.26247	1.72485	8.79363
H	6.80203	1.24493	9.69534
H	7.73612	2.65668	10.21207
C	10.07387	0.53181	4.53183
H	10.61542	-0.12670	3.85561
C	8.55341	1.31135	6.03981
H	7.68789	1.35430	6.69464
C	5.34548	3.56474	9.25615
H	5.72464	4.21270	10.06241
H	4.76082	2.75624	9.72273
H	4.65727	4.16769	8.64657
C	4.28409	-0.38390	5.84915
H	3.90021	0.64060	5.95971
H	4.64923	-0.71217	6.83562
H	3.43812	-1.03317	5.57051
C	8.76475	6.66285	3.72999
H	8.87907	7.66863	4.16517
H	8.59270	6.80287	2.65165
H	9.71744	6.12686	3.85645
C	8.91353	0.18917	5.26579
H	8.38897	-0.76230	5.22748
C	7.18189	4.38297	6.36544

References

1. P. Zark, A. Schäfer, A. Mitra, D. Haase, W. Saak, R. West and T. Müller, *J. Organomet. Chem.*, 2010, **695**, 398-408
2. C. Lorber, in *Comprehensive Organometallic Chemistry III*, ed. R. H. Crabtree, Elsevier, Oxford, 2007, pp. 1-60.
3. N. F. Chilton, R. P. Anderson, L. D. Turner, A. Soncini and K. S. Murray, *J. Comput. Chem.*, **2013**, *34*, 1164.
4. S. Stoll, A. Schweiger, *J. Magn. Reson.* **2006**, *178*, 42-55.
5. T. A. Jackson, J. Krzystek, A. Ozarowski, G. B. Wijeratne, B. F. Wicker, D. J. Mindiola and J. Telser, *Organometallics*, 2012, **31**, 8265-8274.
6. TURBOMOLE V6.6 2014 (V7.0 2016), a development of University of Karlsruhe and Forschungszentrum Karlsruhe GmbH, 1989-2007, TURBOMOLE GmbH, since 2007; available from http://www.turbomole.com.
7. ADF2014, SCM, Theoretical Chemistry, Vrije Universiteit, Amsterdam, The Netherlands, http://www.scm.com
8. M. J. Frisch, G. W. Trucks, H. B. Schlegel, G. E. Scuseria, M. A. Robb, J. R. Cheeseman, G. Scalmani, V. Barone, B. Mennucci, G. A. Petersson, H. Nakatsuji, M. Caricato, X. Li, H. P. Hratchian, A. F. Izmaylov, J. Bloino, G. Zheng, J. L. Sonnenberg, M. Hada, M. Ehara, K. Toyota, R. Fukuda, J. Hasegawa, M. Ishida, T. Nakajima, Y. Honda, O. Kitao, H. Nakai, T. Vreven, Jr, J. E. Peralta, F. Ogliaro, M. Bearpark, J. J. Heyd, E. Brothers, K. N. Kudin, V. N. Staroverov, R. Kobayashi, J. Normand, K. Raghavachari, A. Rendell, J. C. Burant, S. S. Iyengar, J. Tomasi, M. Cossi, N. Rega, J. M. Millam, M. Klene, J. E. Knox, J. B. Cross, V. Bakken, C. Adamo, J. Jaramillo, R. Gomperts, R. E. Stratmann, O. Yazyev, A. J. Austin, R. Cammi, C. Pomelli, J. W. Ochterski, R. L. Martin, K. Morokuma, V. G. Zakrzewski, G. A. Voth, P. Salvador, J. J. Dannenberg, S. Dapprich, A. D. Daniels, Farkas, J. B. Foresman, J. V. Ortiz, J. Cioslowski and D. J. Fox, Gaussian 09 Revision D.01, Gaussian Inc. , Wallingford CT, 2009.
9. NBO 5.9. E. D. Glendening, J. K. Badenhoop, A. E. Reed, J. E. Carpenter, J. A. Bohmann, C. M. Morales, and F. Weinhold, (Theoretical Chemistry Institute, University of Wisconsin, Madison, WI, 2011); http://www.chem.wisc.edu/~nbo5